Detection Methods Based on Structured Covariance Matrices for Multivariate SAR Images Processing

R. Ben Abdallah[1], A. Mian[2], A. Breloy[1], A. Taylor[3], M. N. El Korso[1], D. Lautru[1]

***Abstract*—Testing the similarity of covariance matrices from groups of observations has been shown to be a relevant approach for change and/or anomaly detection in synthetic aperture radar images. While the term "similarity" usually refers to equality or proportionality, we explore the testing of shared properties in the structure of low rank plus identity covariance matrices, which are appropriate for radar processing. Specifically, we derive two new generalized likelihood ratio tests to infer i) on the equality of the low rank signal component of covariance matrices, and ii) on the proportionality of the low rank signal component of covariance matrices. The formulation of the second test involves non-trivial optimization problems for which we tailor efficient Majorization-Minimization algorithms. Eventually, the proposed detection methods enjoy interesting properties, that are illustrated on simulations and on an application to real data for change detection.**

***Index Terms*—GLRT, covariance testing, low rank structure, SAR, change detection.**

I. Introduction

Statistical testing of covariance matrix (CM) equality (or proportionality) has received increasing interest in the context of synthetic aperture radar (SAR) image processing. Indeed, this well established hypothesis test has been successfully studied and applied to change/anomaly detection and classification in SAR images. Notably, equality testing has been proposed for change detection in SAR in [1]–[8]. A clear overview and statistical analysis of this topic is proposed in [9]. The extension to proportionality testing has been proposed in [10], [11]. In this scope, elliptical noise modeling has also been studied to develop robust CM-based SAR image processing in [12]–[15].

In this paper, we propose new statistical tests in the context of structured CM. Indeed, the CM of radar measurements usually exhibit inherent structures. In a very general case, the samples can be modeled as a realizations of a low rank (LR) signal component plus white Gaussian (thermal) noise. This leads to a CM structured as $\mathbf{\Sigma} = \mathbf{\Sigma}_R + \sigma^2\mathbf{I}$, where $\mathbf{\Sigma}_R$ is the LR signal CM. Taking this prior knowledge in the detection process offers several advantages: i) introducing relevant prior information (here, the LR CM structure) in the model improves detection performances; ii) LR structured models allow to deal with low sample support issues, since less samples are required to estimate the CM. Especially, it allows to perform tests even when the sample covariance matrix (SCM) is not invertible, while this condition is restrictive for standard tests; iii) the considered formulation can go beyond equality and proportionality testing. For example, consider local power fluctuations of ground response modeled as $\mathbf{\Sigma}_i = \tau_i\mathbf{\Sigma}_R + \sigma^2\mathbf{I}$, where $\tau_i \in \mathbb{R}^+$ and i denotes the index of a homogeneous set. Such model leads to $\mathbf{\Sigma}_i \neq \mathbf{\Sigma}_j$ as well as $\mathbf{\Sigma}_i \not\propto \mathbf{\Sigma}_j$ for $i \neq j$. If the goal is to detect a signal anomaly in $\mathbf{\Sigma}_R$, detectors based on CM equality/proportionality testing may lead to an excessive number of false alarms.

Specifically, we propose two novel Generalized Likelihood Ratio Tests (GLRT) that account for the considered LR structure, with assumed known rank. Formally, these detectors re-express the equality and proportionality tests, but only on the signal LR component $\mathbf{\Sigma}_R$ of the total CM. The derivation of the second test requires to solve some non-trivial optimization problems, for which we tailor appropriate Majorization-Minimization (MM) algorithms in the supplementary materials attached to this paper. It is worth mentioning that the proposed formulations and optimization methods can also be adapted to design various other tests - such as eigenvectors (or principal subspace) equality testing - for other specific applications.

Finally, the performance of the proposed detectors are illustrated on simulated data, where they exhibit interesting properties. Furthermore, the benefits of the proposed methods are also illustrated for a change detection application on a UAVSAR dataset (courtesy of NASA/JPL-Caltech, https://uavsar.jpl.nasa.gov). For this application, our conclusions are the following: i) incorporating the LR structure in CM equality testing offers an improvement of the detection performance (especially for small local windows) with a small increase in the computational cost; ii) testing the CM proportionality (either with LR or full rank model) requires more computational time, which does not appear to be beneficial to obtain a high probability detection (PD). This is due to the fact that these detectors are designed to be insensitive to power fluctuations, while this phenomenon is relevant in change detection. However, these detectors are still interesting for a number of other purposes, such as ensuring a low PFA in local anomaly detection [10]; iii) both of the LR methods allow to increase the spatial resolution of the detection process, as they are defined for lower sample support.

Notations: italic type indicates a scalar quantity, lower case boldface indicates a vector quantity and upper case boldface a matrix. The transpose conjugate operator is ^{H}. $\mathrm{Tr}\{\ \}$ and $|\ |$ are respectively the trace and the determinant operators. $\mathrm{etr}\{.\}$ is the exponential of trace operator. $\{w_n\}_{n\in[\![1,N]\!]}$ denotes the set of elements w_n, with $n \in [\![1, N]\!]$, often contracted in

R. Ben Abdallah, A. Breloy, M. N. El Korso, and D. Lautru are with LEME (EA 4416)), University Paris Nanterre. A. Mian is with SONDRA, CentraleSupélec, Université Paris-Saclay, F-91190, Gif-sur-Yvette, France. A. Taylor is with DEMR, ONERA, Université Paris Saclay, F-91123 Palaiseau Cedex, France. Part of this work was supported by ANR-ASTRID MARGARITA (ANR-17-ASTR-0015).

$\{w_n\}$. Definition of needed eigenvalue decomposition will be through the equality symbol $\overset{\text{EVD}}{=}$. $\mathcal{H}_M^{++}$ denotes the set of $M \times M$ Hermitian positive definite matrices. $\propto$ stands for "proportional to". $\mathbf{x} \sim \mathcal{CN}(\boldsymbol{\mu}, \boldsymbol{\Sigma})$ is a complex-valued random Gaussian vector of mean $\boldsymbol{\mu}$ and CM $\boldsymbol{\Sigma}$. $x \sim \Gamma(\nu, \xi)$ is a random variable following a Gamma distribution of shape ν and scale ξ.

II. Model and problem statement

1) Signal model: In the following, $\mathbf{z}_k^i$ denotes a sample, in which the superscript $i \in [\![0, I]\!]$ refers to the index of a set of i.i.d. variables, and $k \in [\![1, K_i]\!]$ to the index of the sample in this set (of size K_i). Depending on the context, i may stand either for the index of a local patch, or for the index of a time-series. For a given sample set $\{\mathbf{z}_k^i\}$ of multivariate pixels, we consider the following data model:

$$\mathbf{z}_k^i = \mathbf{s}_k^i + \mathbf{n}_k^i \tag{1}$$

• $\mathbf{s}_k^i$ is the ground response, that consists of a mixture of low rank signal contributions. The resulting observation is modeled as $\mathbf{s}_k^i \sim \mathcal{CN}(\mathbf{0}, \mathbf{C}_i)$ with unknown LR CM $\mathbf{C}_i$. As commonly assumed in the literature [16], [17], the rank R is considered known, or already pre-established[1].
• $\mathbf{n}_k^i \sim \mathcal{CN}(\mathbf{0}, \sigma^2 \mathbf{I}_M)$ is the thermal noise of known variance σ^2. The extension of proposed algorithms to unknown σ^2 is trivial and is tested on real data in section V.
Consequently, the samples are distributed as $\mathbf{z}_k^i \sim \mathcal{CN}(\mathbf{0}, \boldsymbol{\Sigma}_i)$ where the total CM has a LR plus identity structure. To reflect this structure, we consider the following parameterization:

$$\boldsymbol{\Sigma}_i = \tau_i \mathbf{V}_i \boldsymbol{\Lambda}_i \mathbf{V}_i^H + \sigma^2 \mathbf{I} \triangleq \tau_i \boldsymbol{\Sigma}_R^i + \sigma^2 \mathbf{I} \tag{2}$$

where τ_i is a positive scaling factor, $\mathbf{V}_i$ is a $M \times R$ unitary matrix, $\boldsymbol{\Lambda}_i$ is a $R \times R$ positive diagonal matrix. Eventually, the likelihood of the dataset is

$$\mathcal{L}(\{\mathbf{z}_k^i\}|\boldsymbol{\theta}) = \prod_{i=0}^{I} \frac{\text{etr}\{-\mathbf{S}_i \boldsymbol{\Sigma}_i^{-1}(\boldsymbol{\theta})\}}{|\ \boldsymbol{\Sigma}_i(\boldsymbol{\theta})\ |^{K_i}} \tag{3}$$

with $\mathbf{S}_i = \sum_{k=1}^{K_i} \mathbf{z}_k^i \mathbf{z}_k^{iH}$ and where $\boldsymbol{\theta}$ denotes the set of parameters defining the $\boldsymbol{\Sigma}_i$'s (specified in the following). Notice that this model generalizes the LR compound Gaussian plus white Gaussian noise distribution, that is a realistic model for radar measurements embedded in thermal noise [17], [22]. The latter corresponds to the special case $K_i = 1, \forall i \in [\![0, I]\!]$ in our setting.

2) Problem statement: For the general model in (2)-(3), we turn to the problem of testing whether the CM of the sample set under test $i = 0$ shares some common properties with the secondary sets $i \in [\![1, I]\!]$. These properties are related to the parameters of the decomposition in (2) (i.e. τ_i, $\mathbf{V}_i$, and $\boldsymbol{\Lambda}_i$) and will be specified depending on the proposed test. This problem is relevant to detect e.g., a local anomaly in the patch w.r.t. adjacent patches, or a temporal change in the last sample of a time-series.

[1] Indeed, the proposed results can still be applied using plug-in rank estimates or by integrating physical prior knowledge on this parameter [18]. About rank estimation, the reader is refered to the overview [19] and recent methods using shrinkage [20] or random matrix theory [21].

III. State of the art: existing GLRTs

1) Equality testing: the standard hypothesis test [9] reads

$$\begin{cases} \mathcal{H}_0 : \ \boldsymbol{\Sigma}_0 = \boldsymbol{\Sigma},\ \boldsymbol{\Sigma}_i = \boldsymbol{\Sigma}\ \forall i \in [\![1, I]\!] \\ \mathcal{H}_1 : \ \boldsymbol{\Sigma}_0 \neq \boldsymbol{\Sigma},\ \boldsymbol{\Sigma}_i = \boldsymbol{\Sigma}\ \forall i \in [\![1, I]\!] \end{cases} \tag{4}$$

The GLRT for this hypothesis test, denoted $t_{\text{glr}}^{\text{E}}$, reads

$$|\hat{\boldsymbol{\Sigma}}_{\mathcal{H}_0}| / \left(|\hat{\boldsymbol{\Sigma}}_{\mathcal{H}_1}^0|^{\rho_0} |\hat{\boldsymbol{\Sigma}}_{\mathcal{H}_1}^\star|^{\rho_\star} \right) \underset{\mathcal{H}_0}{\overset{\mathcal{H}_1}{\gtrless}} \delta_{\text{glr}}^{\text{E}}, \tag{5}$$

with the quantities $K = \sum_{i=0}^{I} K_i$, $K_\star = K - K_0$, the ratios $\rho_0 = K_0/K$, $\rho_\star = K_\star/K$, and the SCMs $\hat{\boldsymbol{\Sigma}}_{\mathcal{H}_0} = \sum_{i=0}^{I} \mathbf{S}_i/K$, $\hat{\boldsymbol{\Sigma}}_{\mathcal{H}_1}^0 = \mathbf{S}_0/K_0$ and $\hat{\boldsymbol{\Sigma}}_{\mathcal{H}_1}^\star = \sum_{i=1}^{I} \mathbf{S}_i/K_\star$.

2) Proportionality testing: The classical hypothesis test [10] is

$$\begin{cases} \mathcal{H}_0 : \ \boldsymbol{\Sigma}_0 = \beta_0 \boldsymbol{\Sigma},\ \boldsymbol{\Sigma}_i = \beta_i \boldsymbol{\Sigma}\ \forall i \in [\![1, I]\!] \\ \mathcal{H}_1 : \ \boldsymbol{\Sigma}_0 \neq \beta_0 \boldsymbol{\Sigma},\ \boldsymbol{\Sigma}_i = \beta_i \boldsymbol{\Sigma}\ \forall i \in [\![1, I]\!] \end{cases} \tag{6}$$

The GLRT on proportionality, denoted $t_{\text{glr}}^{\text{P}}$, is given as:

$$\left(\frac{|\hat{\beta}_{\mathcal{H}_0}^0 \hat{\boldsymbol{\Sigma}}_{\mathcal{H}_0}^{\text{gfp}}|}{|\hat{\boldsymbol{\Sigma}}_{\mathcal{H}_1}^0|} \right)^{K_0} \prod_{i=1}^{I} \left(\frac{|\hat{\beta}_{\mathcal{H}_0}^i \hat{\boldsymbol{\Sigma}}_{\mathcal{H}_0}^{\text{gfp}}|}{|\hat{\beta}_{\mathcal{H}_1}^i \hat{\boldsymbol{\Sigma}}_{\mathcal{H}_1}^{\text{gfp}}|} \right)^{K_i} \underset{\mathcal{H}_0}{\overset{\mathcal{H}_1}{\gtrless}} \delta_{\text{glr}}^{\text{P}}, \tag{7}$$

where $\{\hat{\beta}_{\mathcal{H}_0}^i\}$ and $\hat{\boldsymbol{\Sigma}}_{\mathcal{H}_0}^{\text{gfp}}$ are proportionality coefficients and shape matrix estimated with the generalized fixed point estimator (GFPE) [11] applied on the set $\{\mathbf{S}_i\}_{i \in [\![0,I]\!]}$, $\{\hat{\beta}_{\mathcal{H}_1}^i\}$ and $\hat{\boldsymbol{\Sigma}}_{\mathcal{H}_1}^{\text{gfp}}$ are obtained from the GFPE on the set $\{\mathbf{S}_i\}_{i \in [\![1,I]\!]}$, and where $\hat{\boldsymbol{\Sigma}}_{\mathcal{H}_1}^0$ is the SCM defined above.

IV. Proposed detectors

A. GLRT for LR CM equality testing

In this section, we develop a GLRT that is sensitive to a variation of any parameter of the LR signal CM in the set $i = 0$. Thus, for the CM model in (2), consider the following hypothesis test:

$$\begin{cases} \mathcal{H}_0 : \ \left| \tau_i \boldsymbol{\Sigma}_R^i = \boldsymbol{\Sigma}_R\ \forall i \in [\![0, I]\!] \right. \\ \mathcal{H}_1 : \ \begin{vmatrix} \tau_i \boldsymbol{\Sigma}_R^i = \boldsymbol{\Sigma}_R\ \forall i \in [\![1, I]\!] \\ \tau_0 \boldsymbol{\Sigma}_R^0 \neq \boldsymbol{\Sigma}_R, \end{vmatrix} \end{cases} \tag{8}$$

that reads almost identical to the standard equality testing of section III, except that the CMs belong to the set of LR plus identity structured matrices $\mathcal{S}_{LR}^{++}$. Hence, the hypothesis test can be recasted as

$$\begin{cases} \mathcal{H}_0 : \ \left| \boldsymbol{\Sigma}_i = \boldsymbol{\Sigma}_{R,\mathcal{H}_0} + \sigma^2 \mathbf{I} \ \triangleq\ \boldsymbol{\Sigma}_{\mathcal{H}_0} \in \mathcal{S}_{LR}^{++},\ \forall i \in [\![0, I]\!] \right. \\ \mathcal{H}_1 : \ \begin{vmatrix} \boldsymbol{\Sigma}_0 = \boldsymbol{\Sigma}_{R,\mathcal{H}_1}^0 + \sigma^2 \mathbf{I} \ \triangleq\ \boldsymbol{\Sigma}_{\mathcal{H}_1}^0 \in \mathcal{S}_{LR}^{++} \\ \boldsymbol{\Sigma}_i = \boldsymbol{\Sigma}_{R,\mathcal{H}_1}^\star + \sigma^2 \mathbf{I} \ \triangleq\ \boldsymbol{\Sigma}_{\mathcal{H}_1}^\star \in \mathcal{S}_{LR}^{++},\ \forall i \in [\![1, I]\!] \end{vmatrix} \end{cases}$$

The expression of the GLRT is therefore

$$\frac{\max_{\boldsymbol{\theta}_{\mathcal{H}_1}^{\text{lrE}}} \mathcal{L}(\{\mathbf{z}_k^i\}|\mathcal{H}_1, \boldsymbol{\theta}_{\mathcal{H}_1}^{\text{lrE}})}{\max_{\boldsymbol{\theta}_{\mathcal{H}_0}^{\text{lrE}}} \mathcal{L}(\{\mathbf{z}_k^i\}|\mathcal{H}_0, \boldsymbol{\theta}_{\mathcal{H}_0}^{\text{lrE}})} \underset{\mathcal{H}_0}{\overset{\mathcal{H}_1}{\gtrless}} \delta_{\text{glr}}^{\text{lrE}}, \tag{9}$$

with sets $\boldsymbol{\theta}_{\mathcal{H}_1}^{\text{lrE}} = \left\{ \boldsymbol{\Sigma}_{\mathcal{H}_1}^0, \boldsymbol{\Sigma}_{\mathcal{H}_1}^\star \right\}$ and $\boldsymbol{\theta}_{\mathcal{H}_0}^{\text{lrE}} = \{\boldsymbol{\Sigma}_{\mathcal{H}_0}\}$. In the context of Gaussian data, the MLE of LR structured CM is

obtained by thresholding the eigenvalues of the SCM [16] with the operator $\mathcal{T}_R$. This operator associates to any Hermitian matrix $\mathbf{\Sigma} \overset{\text{EVD}}{=} \mathbf{V}\mathbf{\Lambda}\mathbf{V}^H$ the regularization $\mathcal{T}_R\{\mathbf{\Sigma}\} \overset{\text{EVD}}{=} \mathbf{V}\tilde{\mathbf{\Lambda}}\mathbf{V}^H$ with

$$[\tilde{\mathbf{\Lambda}}]_{i,i} = \begin{cases} \max([\mathbf{\Lambda}]_{i,i}, \sigma^2), & i \leq R \\ \sigma^2, & i > R \end{cases} \tag{10}$$

Therefore it can be easily shown that

$$\hat{\boldsymbol{\theta}}^{\text{lrE}}_{\mathcal{H}_0} = \left\{\mathcal{T}_R\{\hat{\mathbf{\Sigma}}_{\mathcal{H}_0}\}\right\} \text{ and } \hat{\boldsymbol{\theta}}^{\text{lrE}}_{\mathcal{H}_1} = \left\{\mathcal{T}_R\{\hat{\mathbf{\Sigma}}^0_{\mathcal{H}_1}\}, \mathcal{T}_R\{\hat{\mathbf{\Sigma}}^\star_{\mathcal{H}_1}\}\right\}$$

with $\hat{\mathbf{\Sigma}}_{\mathcal{H}_0}$, $\hat{\mathbf{\Sigma}}^0_{\mathcal{H}_1}$ and $\hat{\mathbf{\Sigma}}^\star_{\mathcal{H}_1}$ defined in III. Finally, the GLRT for testing the equality of LR structured matrices, denoted $t^{\text{lrE}}_{\text{glr}}$, reads as:

$$\mathcal{L}(\{\mathbf{z}^i_k\}|\mathcal{H}_1, \hat{\boldsymbol{\theta}}^{\text{lrE}}_{\mathcal{H}_1}) / \mathcal{L}(\{\mathbf{z}^i_k\}|\mathcal{H}_0, \hat{\boldsymbol{\theta}}^{\text{lrE}}_{\mathcal{H}_0}) \underset{\mathcal{H}_0}{\overset{\mathcal{H}_1}{\gtrless}} \delta^{\text{lrE}}_{\text{glr}} \tag{11}$$

To evaluate this test, three SVDs of SCMs are required. In comparison, t^E_{glr} requires to compute the determinant of the same three SCMs. The proposed t^{lrP}_{glr} is therefore slightly computationally more expensive.

B. GLRT for LR CM proportionality testing

In this section, we derive a GLRT to infer on the proportionality of the LR signal component of the CM. Notice that this test differs from strict proportionality testing. Indeed, scaling fluctuations should only apply on the LR part of the signal CM, and not to the identity, related to the thermal noise. For the CM model in (2), this leads to the following hypothesis test

$$\begin{cases} \mathcal{H}_0 : \left| \mathbf{\Sigma}^i_R = \mathbf{\Sigma}_R \ \forall i \in [\![0, I]\!] \right. \\ \mathcal{H}_1 : \left| \begin{array}{l} \mathbf{\Sigma}^i_R = \mathbf{\Sigma}_R \ \forall i \in [\![1, I]\!] \\ \mathbf{\Sigma}^0_R \neq \mathbf{\Sigma}_R \end{array} \right. \end{cases} \tag{12}$$

which reads as signals sharing the same CM structure, but with fluctuating power τ_i w.r.t. sample set i. The test (12) can be recasted as:

$$\begin{cases} \mathcal{H}_0 : \left| \mathbf{\Sigma}_i = \tau_i \mathbf{V}_{\mathcal{H}_0} \mathbf{\Lambda}_{\mathcal{H}_0} (\mathbf{V}_{\mathcal{H}_0})^H + \sigma^2 \mathbf{I}, \ \forall i \in [\![0, I]\!] \right. \\ \mathcal{H}_1 : \left| \begin{array}{l} \mathbf{\Sigma}_0 = \ \mathbf{V}^0_{\mathcal{H}_1} \mathbf{A}^0_{\mathcal{H}_1} (\mathbf{V}^0_{\mathcal{H}_1})^H + \sigma^2 \mathbf{I} \\ \mathbf{\Sigma}_i = \tau_i \mathbf{V}^\star_{\mathcal{H}_1} \mathbf{\Lambda}^\star_{\mathcal{H}_1} (\mathbf{V}^\star_{\mathcal{H}_1})^H + \sigma^2 \mathbf{I}, \ \forall i \in [\![1, I]\!] \end{array} \right. \end{cases} \tag{13}$$

where we collapsed a redundant parameter as $\mathbf{A}_0 = \tau_0 \mathbf{\Lambda}_0$ (that is still diagonal). The expression of the corresponding GLRT, denoted $t^{\text{lrP}}_{\text{glr}}$ is given by:

$$\frac{\max_{\boldsymbol{\theta}^{\text{lrP}}_{\mathcal{H}_1}} \ \mathcal{L}(\{\mathbf{z}^i_k\}|\mathcal{H}_1, \boldsymbol{\theta}^{\text{lrP}}_{\mathcal{H}_1})}{\max_{\boldsymbol{\theta}^{\text{lrP}}_{\mathcal{H}_0}} \ \mathcal{L}(\{\mathbf{z}^i_k\}|\mathcal{H}_0, \boldsymbol{\theta}^{\text{lrP}}_{\mathcal{H}_0})} \underset{\mathcal{H}_0}{\overset{\mathcal{H}_1}{\gtrless}} \delta^{\text{lrP}}_{\text{glr}}, \tag{14}$$

with sets of parameters $\boldsymbol{\theta}^{\text{lrP}}_{\mathcal{H}_0} = \left\{\{\tau_i\}_{i \in [\![0,I]\!]}, \mathbf{V}_{\mathcal{H}_0}, \mathbf{\Lambda}_{\mathcal{H}_0}\right\}$ and $\boldsymbol{\theta}^{\text{lrP}}_{\mathcal{H}_1} = \left\{\{\tau_i\}_{i \in [\![1,I]\!]}, \mathbf{V}^\star_{\mathcal{H}_1}, \mathbf{\Lambda}^\star_{\mathcal{H}_1}, \mathbf{V}^0_{\mathcal{H}_1}, \mathbf{A}^0_{\mathcal{H}_1}\right\}$. It is clear that the maximization of the likelihood function is not trivial, due notably to the unitary constraints on the eigenvectors. To overcome this issue, we propose the use of the block-MM algorithm [23]. This methodology can be applied to our problem by generalizing some results of [22]. Due to space constraints, the full derivation of the proposed algorithms is left in the supplementary material attached to this paper. Eventually, these algorithms allow to evaluate the MLEs $\hat{\boldsymbol{\theta}}^{\text{lrP}}_{\mathcal{H}_0}$ and $\hat{\boldsymbol{\theta}}^{\text{lrP}}_{\mathcal{H}_1}$ and the GLRT as

$$\mathcal{L}(\{\mathbf{z}^i_k\}|\mathcal{H}_1, \hat{\boldsymbol{\theta}}^{\text{lrP}}_{\mathcal{H}_1}) / \mathcal{L}(\{\mathbf{z}^i_k\}|\mathcal{H}_0, \hat{\boldsymbol{\theta}}^{\text{lrP}}_{\mathcal{H}_0}) \underset{\mathcal{H}_0}{\overset{\mathcal{H}_1}{\gtrless}} \delta^{\text{lrP}}_{\text{glr}} \tag{15}$$

In terms of computational cost, it is noted that each update of our proposed MM algorithm is obtained in closed form. Empirically, this algorithm converges quite fast, and we used only 10 iterations in our application to real data. The main bottleneck is in the update of the eigenvectors, which requires to compute thin-SVD of an $M \times R$ matrix. Thus, this test is more computationally expensive than t^E_{glr} or t^{lrP}_{glr}. However, it is on the same scale as its full rank counterpart t^P_{glr}, which involves fixed point iterations of SCMs inversions.

V. Simulations and application

A. Numerical simulations

In this section, the performance of the aforementioned detectors is illustrated through simulations. We use as a criteria the receiver operating characteristic (ROC) curve which displays the probability of detection (PD) versus the probability of false alarm (PFA).

1) Simulation setup: We consider $M = 20$, $R = 5$, $K_i = 25 \ \forall i$ with $I = 3$. The sample set $\{z^i_k\}$ is generated according to $\mathbf{z}^i_k \sim \mathcal{CN}(\mathbf{0}, \mathbf{\Sigma}_i)$ with $\mathbf{\Sigma}_i$ given in (2): $\mathbf{V}_i$ are the first R eigenvectors of the Toeplitz matrix $[\mathbf{\Sigma}_T]_{i,j} = \rho^{|i-j|}$ with $\rho = 0.9(1+\sqrt{-1})/\sqrt{2}$ and $[\mathbf{\Lambda}_i]_{r,r} = \alpha(R+1-r)$, where α is set so that the signal to noise ratio fits $\text{SNR} = \text{Tr}\{\mathbf{\Lambda}_i\}/R\sigma^2 = 15\text{dB}$ with $\sigma^2 = 1$. The variable τ_i is specified below for each scenario. Under $\mathcal{H}_1$, the anomaly in the LR signal CM of the set $i = 0$ is generated by either $i)$ reversing the eigenvalues, i.e. $[\mathbf{\Lambda}_0]_{r,r} = \alpha r$ ("*structure change*"); or $ii)$ changing one of the eigenvectors in $\mathbf{V}_i$ ("*subspace change*"). Note that the structure change is more challenging since a subspace change is easier to detect at high SNR. In order to compute the ROC curves, 10^4 Monte-Carlo runs are performed under both $\mathcal{H}_0$ and $\mathcal{H}_1$ and the PD and PFA are computed w.r.t. a threshold grid for each detector.

2) Compared detectors: We compare the following detection statistics: the GLRT for equality testing $t^{\text{E}}_{\text{glr}}$ from Section III-1, the GLRT for proportionality testing $t^{\text{P}}_{\text{glr}}$ from Section III-2, the proposed GLRT for LR equality testing $t^{\text{lrE}}_{\text{glr}}$ from Section IV-A, and the proposed GLRT for LR proportionality testing $t^{\text{lrP}}_{\text{glr}}$ from Section IV-B.

3) Results: Figure 1 displays the ROC curves of the detectors for the signal model from section IV-A (homogeneous power), i.e. $\tau_i = 1 \ \forall i$. Under this settings, the performance of $t^{\text{E}}_{\text{glr}}$ and $t^{\text{P}}_{\text{glr}}$ are almost identical. The same observation is made for $t^{\text{lrE}}_{\text{glr}}$ and $t^{\text{lrP}}_{\text{glr}}$, which both outperform their full rank counterparts since they exploit the LR structure of the CM appropriately. Figure 2 displays the ROC curves of the detectors for the signal model from section IV-B (fluctuating power) with $\tau_i \sim \Gamma(\nu, 1/\nu)$ and $\nu = 1$. Under this settings $t^{\text{lrP}}_{\text{glr}}$ exhibits the best performance, as expected. This is mainly due to a high false alarm rate of the other detectors, as the fluctuation of the signal power generates CMs that are not equal, nor proportional, even under $\mathcal{H}_0$. Hence, $t^{\text{lrP}}_{\text{glr}}$ appears

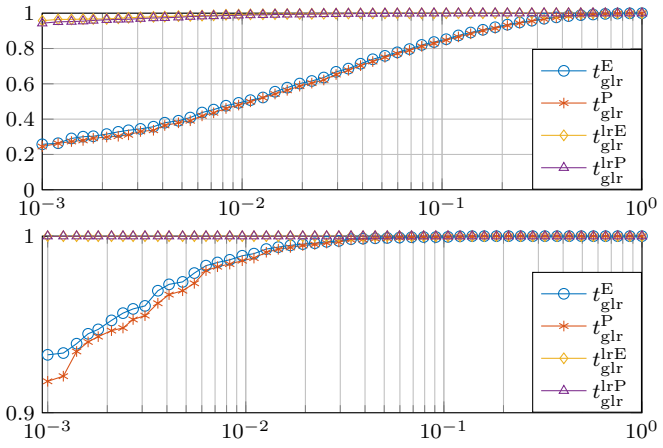

Figure 1: ROC curves for the model in IV-A: $\mathcal{H}_1$ is either a structure change (top) or a subspace change (bottom).

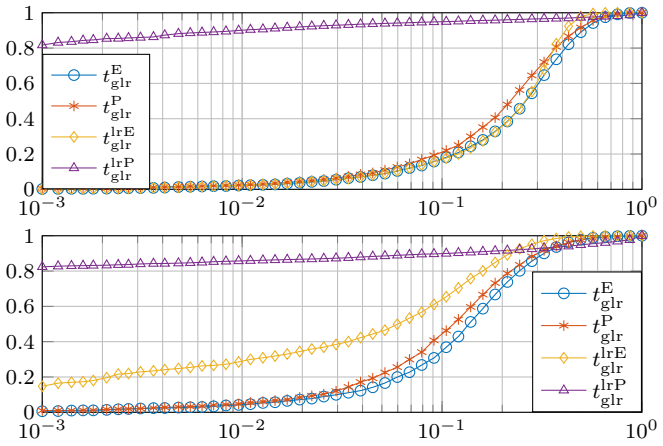

Figure 2: ROC curves for the model in IV-B. $\mathcal{H}_1$ is either a structure change (top) or a subspace change (bottom).

interesting for reducing the false alarms rate when the signal has a varying power over the observed sets.

B. Change detection on real data

In this section, the performance of the proposed detectors is illustrated for change detection on a UAVSAR dataset.

1) Setup: The considered dataset is SanAnd_26524_03 Segment 4, of coordinates (top left pixel) $[2891, 28891]$, with 2 acquisition dates : April 23, 2009 and May 11, 2015. For one acquisition, the initial datacube size is $2360 \times 600 \times 3$ and is pre-processed using the wavelet-decomposition transform presented in [24]. This transformation, which allows to decompose a SAR image into canals corresponding to a physical behaviour of the scatterers, has been shown to increase the detection performance [24]. This transformation increases the depth of the datacube from $M = 3$ to $M = 12$. To form local patches, we use a 5×5 sliding window centered around each pixel. As $I = 2$, these patches provide two sets: $\{\mathbf{z}_k^0\}$ and $\{\mathbf{z}_k^1\}$ with $k \in [\![1, 25]\!]$. The different presented detectors are then applied on these two sets to test a change in the properties/parameters of the CM between $i = 0$ and $i = 1$.

The ground truth for change detection is taken from [25] and presented in Figure 3. This provides observations under both $\mathcal{H}_0$ and $\mathcal{H}_1$, which allows us to compute the ROC curves empirically.

2) Compared detectors: We compare the same detectors as in the previous section. The proposed LR detection methods are applied with $R = 1$, as a rank one signal component can be assumed by analyzing the spectrum of the data matrix. This simplification still allows to obtain interesting results in average, and the use of local adaptive rank selection is left as a potential extension. The noise variance σ^2 is estimated locally with the mean of the $(M - 1)$ lowest eigenvalues computed with a SVD of the SCM of all samples $\{\mathbf{z}_k^i\}$ in the patch. To show the benefits of the multivariate setting, we also compare the results with a monovariate detector applied to the summed entries of each pixel, denoted t_m, as well as the so-called normalized mean-differences detector, denoted t_{Ndiff} [26].

3) Results: The ROC curves of the different detectors are displayed in Figure 4. In this example, $t^{\mathrm{lrE}}_{\mathrm{glr}}$ offers an improvement of the detection performance compared to the standard equality testing $t^{\mathrm{E}}_{\mathrm{glr}}$. This improvement is obtained for only a slight increase in the computational time, highlighting the interest of the proposed LR formulation. $t^{\mathrm{lrP}}_{\mathrm{glr}}$ offers similar performance, but only for low false alarm rate. Thus, for this application, this test may not be worth the increase in the computational time. This is also the case for its counterpart t^{P}_{glr}, which exhibits the lowest performance in this context. Intuitively, a power fluctuation seems interesting to be captured when it comes to change detection. Therefore, proportionality testing (not sensitive to this change) may not be the most appropriate for this application, as illustrated by the performance of $t^{\mathrm{P}}_{\mathrm{glr}}$. However, this detector is still interesting for other purposes, such as local anomaly detection [10].

For each detector, Figure 5 displays the PD w.r.t. the spatial window size $\sqrt{K}$ with fixed $\mathrm{PFA} = 5\%$. Up to a reasonable window size, the detection performance increases w.r.t. K. However, this is at the detriment of the spatial resolution of the process. This figure hence illustrates the interest of the proposed LR methods, as they offer an improvement of the performance/resolution trade-off. Notably, the proposed methods allow for $K < M$, where other standard covariance based detectors are not defined (due to non-invertible SCMs).

VI. Conclusion

This paper proposed two new detectors for CM based detection process. These detectors extend, respectively, the equality and proportionality testing to LR structured CM models, with a mild increase in the computational cost w.r.t. their corresponding full rank counterparts. Numerical simulations illustrated their properties and interest depending on the context. An application to real data for change detection in SAR images time-series showed the interest of the LR approach. Specifically, the LR equality testing offers a gain in detection performance, while the LR proportionality testing does, but only for low PFA. Most notably, both of the proposed LR methods allow to increase the spatial resolution of the detection process, as they require fewer samples than the size of the data.

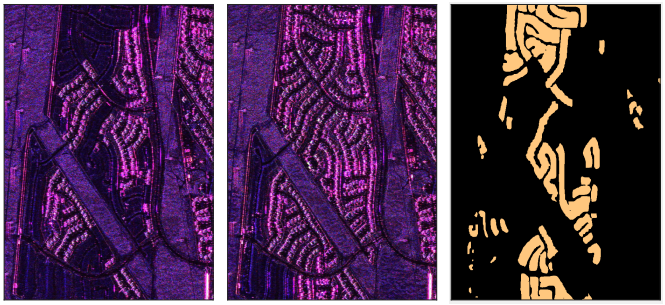

Figure 3: UAVSAR Dataset in Pauli representation. Left: April 23, 2009. Middle: May 15, 2011. Right: Ground Truth for change detection.

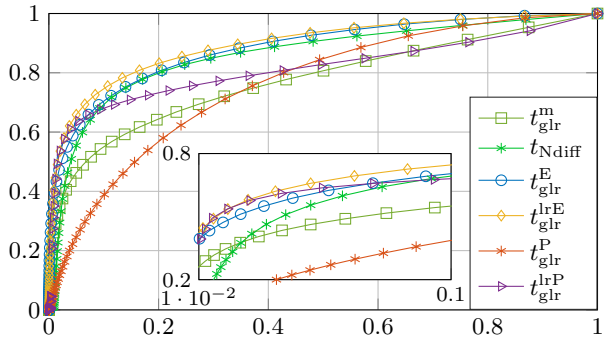

Figure 4: ROC curves (PD versus PFA) of the different detectors on the UAVSAR dataset.

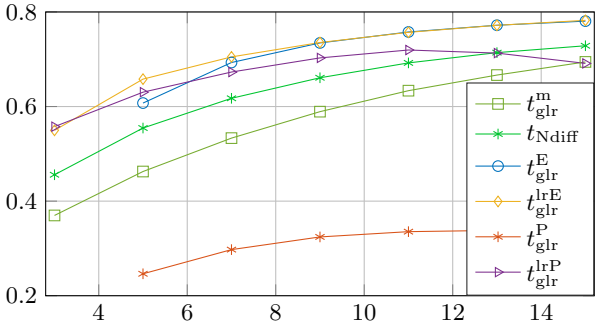

Figure 5: PD versus spatial window size $\sqrt{K}$ for fixed PFA $= 5\%$ of the different detectors on the UAVSAR dataset.

References

[1] K. Conradsen, A. A. Nielsen, J. Schou, and H. Skriver, "A test statistic in the complex wishart distribution and its application to change detection in polarimetric SAR data," *IEEE Transactions on Geoscience and Remote Sensing*, vol. 41, no. 1, pp. 4–19, 2003.

[2] L. M. Novak, "Change detection for multi-polarization multi-pass SAR," *Algorithms for Synthetic Aperture Radar Imagery XII*, vol. 5808, no. 1, pp. 234–247, 2005.

[3] S. W. Chen, X. S. Wang, and M. Sato, "Polinsar complex coherence estimation based on covariance matrix similarity test," *IEEE Transactions on Geoscience and Remote Sensing*, vol. 50, no. 11, pp. 4699–4710, Nov 2012.

[4] M. Liu, H. Zhang, C. Wang, and F. Wu, "Change detection of multilook polarimetric sar images using heterogeneous clutter models," *IEEE Transactions on Geoscience and Remote Sensing*, vol. 52, no. 12, pp. 7483–7494, Dec 2014.

[5] V. Carotenuto, A. De Maio, C. Clemente, and J. Soraghan, "Unstructured versus structured glrt for multipolarization SAR change detection," *IEEE Geoscience and Remote Sensing Letters*, vol. 12, no. 8, pp. 1665–1669, 2015.

[6] A. A. Nielsen, K. Conradsen, and H. Skriver, "Change detection in full and dual polarization, single- and multifrequency sar data," *IEEE Journal of Selected Topics in Applied Earth Observations and Remote Sensing*, vol. 8, no. 8, pp. 4041–4048, Aug 2015.

[7] A. A. Nielsen, K. Conradsen, and H. Skriver, "Omnibus test for change detection in a time sequence of polarimetric SAR data," *IEEE International Geoscience and Remote Sensing Symposium (IGARSS)*, 2016.

[8] A. De Maio, D. Orlando, L. Pallotta, and C. Clemente, "A multifamily glrt for oil spill detection," *IEEE Transactions on Geoscience and Remote Sensing*, vol. 55, no. 1, pp. 63–79, 2017.

[9] D. Ciuonzo, V. Carotenuto, and A. De Maio, "On multiple covariance equality testing with application to SAR change detection," *IEEE Transactions on Signal Processing*, vol. 65, no. 19, pp. 5078–5091, 2017.

[10] A. Taylor, H. Oriot, P. Forster, and F. Daout, "Reducing false alarm rate by testing proportionality of covariance matrices," 2017 International RADAR conference, 2017.

[11] A. Taylor, P. Forster, F. Daout, H. Oriot, and L. Savy, "A generalization of the fixed point estimate for packet-scaled complex covariance matrix estimation," *IEEE Transactions on Signal Processing*, vol. 65, no. 20, pp. 5393–5405, 2017.

[12] G. Vasile, J. P. Ovarlez, F. Pascal, and C. Tison, "Coherency matrix estimation of heterogeneous clutter in high-resolution polarimetric sar images," *IEEE Transactions on Geoscience and Remote Sensing*, vol. 48, no. 4, pp. 1809–1826, April 2010.

[13] P. Formont, F. Pascal, G. Vasile, J.-P. Ovarlez, and L. Ferro-Famil, "Statistical classification for heterogeneous polarimetric SAR images," *IEEE Journal of Selected Topics in Signal Processing*, vol. 5, no. 3, pp. 567–576, 2011.

[14] M. Liu, H. Zhang, and C. Wang, "Change detection in urban areas of high-resolution polarization sar images using heterogeneous clutter models," *3rd International Asia-Pacific Conference on Synthetic Aperture Radar (APSAR)*, 2011.

[15] A. Mian, J-P. Ovarlez, G. Ginolhac, and A.M. Atto, "A robust change detector for highly heterogeneous images," 2018 IEEE International Conference on Acoustics, Speech and Signal Processing, 2018.

[16] B. Kang, V. Monga, and M. Rangaswamy, "Rank-constrained maximum likelihood estimation of structured covariance matrices," *IEEE Transactions on Aerospace and Electronic Systems*, vol. 50, no. 1, pp. 501–515, January 2014.

[17] O. Besson, "Bounds for a mixture of low-rank compound-gaussian and white gaussian noises," *IEEE Transactions on Signal Processing*, vol. 64, no. 21, pp. 5723–5732, Nov 2016.

[18] N. A. Goodman and J. M. Stiles, "On clutter rank observed by arbitrary arrays," *IEEE Transactions on Signal Processing*, vol. 55, no. 1, pp. 178–186, Jan 2007.

[19] P. Stoica and Y. Selen, "Model-order selection: a review of information criterion rules," *IEEE Signal Processing Magazine*, vol. 21, no. 4, pp. 36–47, July 2004.

[20] L. Huang and H. C. So, "Source enumeration via mdl criterion based on linear shrinkage estimation of noise subspace covariance matrix," *IEEE Transactions on Signal Processing*, vol. 61, no. 19, pp. 4806–4821, Oct 2013.

[21] E. Terreaux, J.-P. Ovarlez, and F. Pascal, "Robust model order selection in large dimensional elliptically symmetric noise," *arXiv:1710.06735*.

[22] Y. Sun, A. Breloy, P. Babu, D. P. Palomar, F. Pascal, and G. Ginolhac, "Low-complexity algorithms for low rank clutter parameters estimation in radar systems," *IEEE Transactions on Signal Processing*, vol. 64, no. 8, pp. 1986–1998, April 2016.

[23] Y. Sun, P. Babu, and D. P. Palomar, "Majorization-minimization algorithms in signal processing, communications, and machine learning," *IEEE Transactions on Signal Processing*, vol. 65, no. 3, pp. 794–816, Feb 2017.

[24] A. Mian, J.-P. Ovarlez, G. Ginolhac, and A. Atto, "Multivariate change detection on high resolution monovariate sar image using linear time-frequency analysis," *25th European Signal Processing Conference (EUSIPCO)*, pp. 1942–1946, 2017.

[25] D. Ratha, S. De, T. Celik, and A. Bhattacharya, "Change detection in polarimetric sar images using a geodesic distance between scattering mechanisms," *IEEE Geoscience and Remote Sensing Letters*, vol. 14, no. 7, pp. 1066–1070, July 2017.

[26] P. Villa and G. Lechi, "Normalized difference reflectance: an approach to quantitative change detection," in *2007 IEEE International Geoscience and Remote Sensing Symposium*, July 2007, pp. 2366–2369.